J. Am. Chem. Soc. 1984, 106, 6517-6524

Conclusion

Trimethyl phosphite reacts readily with a variety of nucleophiles in the gas phase. Initial reaction proceeds through formation of an ion–dipole complex to a tetracoordinate phosphoranide intermediate and then to a new ion–dipole complex consisting of the displaced methoxide and the newly-formed neutral. In cases where subsequent reactions are fairly slow, collisional stabilization of the phosphoranide intermediate is possible, and this adduct is observed. If the original nucleophile contains a hydrogen which is labile in the intermediate, then abstraction of this hydrogen by methoxide is the preferred final step in the reaction. When the displacement of methoxide is sufficiently endothermic a competing S_N2 reaction at a methyl carbon by the original nucleophile occurs.

Nucleophiles without an additional labile proton react similarly, but now a more equal competition is established between S_N2 reactions at carbon by the original nucleophile and the displaced methoxide. In addition to products formed by both of these reactions, the relative amounts of which are strongly dependent on the thermodynamics of the ion–dipole complex equilibrium, both methoxide ion and the phosphoranide adduct are now observed.

These results should be applicable to gas-phase electrophilic reactions of tervalent phosphorus in general. We have also examined reactions, similar to those reported here, with triisopropyl phosphite. The results are comparable; the only major difference comes about due to the possibility of elimination of propene from reaction of a strong base with an isopropyloxy group. We intend to continue studying the reactions of phosphorus in the gas phase.

Acknowledgment. We gratefully acknowledge the support of this work by the U.S. Army Research Office under Contract DAAG29-82-K-0025. We thank Jane Van Doren for her assistance in the SIFT studies.

Registry No. $(CH_3O)_3P$, 121-45-9; CH_3NH^-, 54448-39-4; H^-, 12184-88-2; H_2N^-, 17655-31-1; HO^-, 14280-30-9; $CH_2{=}CHCH_2^-$, 1724-46-5; $(CH_3)_2C{=}C(CH_3)CH_2^-$, 91760-20-2; H_2P^-, 22569-71-7; CH_3O^-, 3315-60-4; CP_3O^-, 51679-31-3; $(CH_3)_2N^-$, 34285-60-4; F^-, 16984-48-8; $(CH_3O)_2POH$, 96-36-6; $(CH_3O)_2PNH_2$, 39230-41-6.

Chiroptical Properties of Disulfides. Ab Initio Studies of Dihydrogen Disulfide and Dimethyl Disulfide

Arvi Rauk

Contribution from the Department of Chemistry, University of Calgary, Calgary, Alberta, Canada T2N 1N4. *Received November 29, 1983*

Abstract: The ground- and excited-state electronic structures of H_2S_2 and $(CH_3)_2S_2$ have been investigated as a function of the S–S dihedral angle, ϕ, by using ab initio SCF and CI calculations with a large basis set. The SCF energies for H_2S_2 and $(CH_3)_2S_2$, −796.23280 and −874.24551 hartrees, respectively, are lower than has hitherto been achieved. The cis and trans barriers to hindered rigid rotation are 37.7 and 21.7 kJ/mol, respectively. Equilibrium dihedral angles of 91.3° and 86.5° are interpolated for the two systems. Ionization potentials are calculated to second order in many-body perturbation theory. The nature of the lowest excited singlet state is found to be in accord with predictions based on Bergson's model of the disulfide linkage at all values of ϕ. However, the second and higher excited states change character significantly as a result of avoided crossings of states in the vicinity of $\phi = 70°$ and 120°. Optical rotatory strengths and oscillator strengths are calculated at several values of ϕ, and the relationship to experimental spectroscopic studies on both cyclic and acyclic disulfides is discussed. For the latter compounds, it is found that the rotatory strengths of the two degenerate transitions at the equilibrium geometry, $\phi \simeq 90°$, do not cancel.

In part because of the importance of the disulfide link to the tertiary structures of proteins, considerable experimental and theoretical efforts have been expended in the investigation of molecules which contain the –S—S– unit. The chemical, physical, and spectroscopic properties of disulfides are intimately linked to the torsional dihedral angle, ϕ, which relates the two RSS planes. The Bergson model[1] of the disulfide unit offers a qualitative explanation of many of the properties of disulfides which exhibit a strong dependence on the value of ϕ. Bergson assumed that only the energies of the two highest occupied molecular orbitals (MO's), which consist of the symmetric and antisymmetric combinations of the nonbonding 3p orbitals of sulfur, will show a strong dependence on ϕ. With use of simple overlap considerations, this dependence was shown to have a form very similar to that shown for the MO's, 9a and 8b, in Figure 1. The energetic behavior of the highest occupied MO's immediately suggests an explanation for the twofold rotation barrier and the equilibrium torsion angle of approximately 90°, as well as the observed ϕ dependence of the lowest ionization potential. If one postulates that the lowest excited state of the disulfide chromophore originates from an electronic excitation out of the highest occupied MO into an orbital such as $\sigma_{SS}{}^*$ which does not have a strong ϕ dependence, then the red shift observed for the lowest band in the UV spectrum of simple disulfides as ϕ is distorted from 90° is also explained. Linderberg and Michl[2] have used Bergson's model and have employed semiempirical MO/CI calculations to explain the inherent lack of optical activity of the first transition in acyclic disulfides and the strong angle dependence of the sign of the rotatory strength. They predicted that for a disulfide link with a right-handed twist (P chirality), the sign of the optical activity of the lowest transition is positive if the torsion angle, ϕ, is less than 90° and negative for $\phi > 90°$. According to the Bergson model,[1] the change in sign occurs as the result of the crossing of two electronic states of A and B symmetry to which the rotatory strengths of the transitions are oppositely signed. The accidential degeneracy of the two states and the near cancellation of rotatory strengths

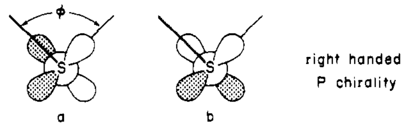

---

[1] Bergson, G. *Ark Kemi* **1958**, *12*, 233–237; **1962**, *18*, 409–434.

[2] Linderberg, J.; Michl, J. *J. Am. Chem. Soc.* **1970**, *92*, 2619–2625.

0002-7863/84/1506-6517$01.50/0

Table I. Ionization Potentials of Dimethyl Disulfide (in eV)

		dihedral angle								
			ϕ = 83.6°			ϕ = 90°			ϕ = 100°	
no.	exptl[a]		IP$_{corr}$[b]	Koopmans[c]		IP$_{corr}$[b]	Koopmans[c]		IP$_{corr}$[b]	Koopmans[c]
1	8.97	13a	8.82	9.23	13a	8.95	9.37	12b	8.74	9.16
2	9.21	12b	9.15	9.59	12b	8.99	9.42	13a	9.17	9.59
3	11.3	12a	11.43	11.78	12a	11.40	11.76	12a	11.36	11.73
4	12.3	11b	12.75	13.19	11b	12.82	13.25	11b	12.91	13.34
5	13.5	11a	14.20	14.56	11a	14.13	14.50	11a	14.03	14.39
6	14.4	10b	15.15	15.78	10b	15.15	15.81	10b	15.19	15.85
7	14.8	10a	15.54	16.17	10a	15.54	16.17	10a	15.55	16.18

[a] Reference 35. [b] Equation 10. [c] $-e_i$.

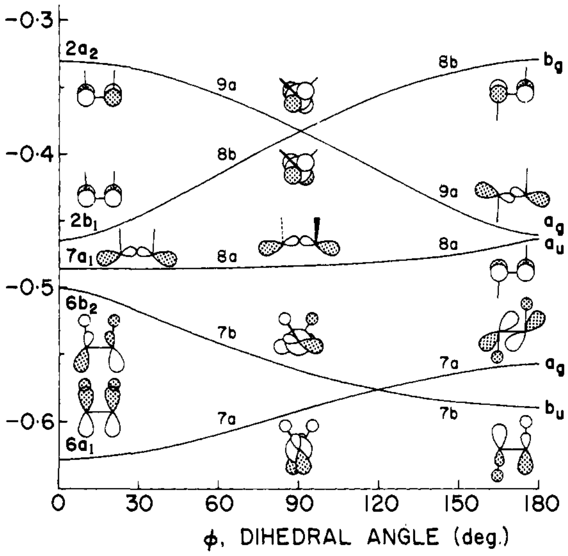

Figure 1. The MO's and MO energies of H_2S_2 as a function of the S–S dihedral angle, ϕ.

near the equilibrium geometry of acyclic disulfides accounts for the inherent lack of optical activity of these compounds.

Richardson and co-workers[3] have calculated the dihedral angle dependence of the rotatory strength of H_2S_2 and $(CH_3)_2S_2$ using semiempirical MO/CI calculations at the CNDO/2 level but with a different parametrization from that used by Linderberg and Michl, and including 3d orbitals on the sulfur atoms. They found a more complicated behavior than expected on the basis of the Bergson model, including a second change of sign of the rotational strength for $\phi < 60°$. There are no investigations at the nonempirical level of the excited-state electronic structures and optical activity of disulfides.

We present below the results of an ab initio MO/CI study of the electronic structures and electronic transition properties, including optical activity, of H_2S_2 and $(CH_3)_2S_2$ and discuss the implications of the results on the available experimental work on these compounds and on disulfides in general.

Experimental Section

The theoretical method employed in the present study has been described in detail elsewhere.[4] Only a brief resume is given below. Partially correlated wave functions are determined to first order by the Rayleigh–Schroedinger perturbation theory

$$\psi_n = \psi_n{}^0 - \sum_j \lambda_{nj}\phi_j{}^0 \tag{1}$$

where

$$\lambda_{nj} = \langle\psi_n{}^0|H|\phi_j{}^0\rangle / (\langle\phi_j{}^0|H|\phi_j{}^0\rangle - \langle\psi_n{}^0|H|\psi_n{}^0\rangle) \tag{2}$$

Here, H is the electronic Hamiltonian operator, $\phi_j{}^0$ is a spin-adapted (singlet) configuration constructed from one or more electron replacements in the Hartree–Fock SCF determinant, ϕ_{HF}, of occupied orbitals by virtual orbitals, and $\psi_n{}^0$ is, in general, a linear combination of quasidegenerate $\phi_l{}^0$ $(l \neq j)$ obtained by diagonalizing a small block of the complete Hamiltonian matrix after regrouping. The function $\psi_n{}^0$ constitutes the "zero-order" part of the wave function, and the set $\phi_j{}^0$ "the first-order correction".

For the ground state, ψ_0, the zero-order part consists of ϕ_{HF}, and all doubly excited configurations, $\phi_k{}^0$, for which $\lambda_{HF,k}$ is greater than a critical value. The first-order corrections are derived from the space of the remaining doubly excited configuration where excitations are allowed from the higher valence orbitals to all except the highest virtual orbitals. A similar procedure is followed for construction of the excited-state wave functions. Initially, the zero-order part consists of an arbitrary number, usually 10 to 15, of the lowest singly excited configurations ordered by energy. To these are added all singly excited configurations which interact strongly with them accoding to eq 2. A limited subspace of triply excited configurations of the type $\phi^0(ij \rightarrow uuv)$ is generated, where $\phi^0(i$ or $j \rightarrow u$ or $v)$ is already in $\psi_n{}^0$, and some of these are incorporated into $\psi_n{}^0$ by the same criterion (eq 2). All matrix elements of the form $\langle\psi_0|\theta|\psi_n\rangle$, where θ is the sum of one-electron operators, are correct to first order.

The one-electron operators of interest are the electric dipole operator, μ, the magnetic dipole operator, m, and the gradient operator, ∇, where

$$\mu = e\mathrm{r} = e\sum_j \mathrm{r}_j \tag{3}$$

$$\mathbf{m} = \frac{\hbar e}{2mci}\sum_j \mathrm{r}_j \times \nabla_j \tag{4}$$

$$\nabla = \sum_j \nabla_j \tag{5}$$

The position and momentum matrix element vectors should be parallel according to

$$\langle\psi_0|\mu|\psi_n\rangle = \frac{\hbar^2}{m(E_n - E_0)}\langle\psi_0|\nabla|\psi_n\rangle \tag{6}$$

which is true for exact wave functions. The angle between the two vector quantities computed by using wave functions in (1) serves as a check on the quality of the wave functions.

As only a small fraction of the total correlation energy is recovered by the present method, the best estimate for the excitation energy is the energy difference between the excited-state energy, correct to second order in the space of all singly excited configurations, and the energy of the Hartree–Fock SCF determinant, ϕ_{HF}. Excitation energies thus derived are cited in Table II and used to obtain the excited-state potential curves plotted in the figures.

A vertical transition between the ground state, ψ_0, and an excited state, ψ_n, is characterized by the oscillator strength, f_{on}, and optical rotatory strength, $[R_{on}]^r$, which are given by

$$f_{on} = 2/3\langle\psi_0|\nabla|\psi_n\rangle\cdot\langle\psi_n|\mathrm{r}|\psi_0\rangle \tag{7}$$

$$[R_{on}]^r = -i\langle\psi_0|\mu|\psi_n\rangle\cdot\langle\psi_n|\mathrm{m}|\psi_0\rangle \tag{8}$$

The origin dependence of $[R_{on}]^r$ may be removed by substitution of eq 6 into eq 8. The resulting expression, described as $[R_{on}]^\nabla$ in Table II is

$$[R_{on}]^\nabla = \frac{e\hbar^2}{m(E_n - E_0)}\langle\psi_0|\nabla|\psi_n\rangle\cdot\langle\psi_n|\mathbf{m}|\psi_0\rangle \tag{9}$$

Ionization potentials are estimated by eq 10 which is obtained by application of the many-body perturbation theory, solved to second order by using the Rayleigh–Schroedinger perturbation theory.[5-8] For ioni-

---

(3) Webb, J.; Strickland, R. W.; Richardson, F. S. *J. Am. Chem. Soc.* **1973**, *95*, 4775–4783.

(4) Rauk, A.; Barriel, J. M. *Chem. Phys.* **1977**, *25*, 409–424.

(5) Pickup, B. T.; Goscinski, O. *Mol. Phys.* **1973**, *26*, 1013–1035.

zation from molecular spin orbital i, with energy e_i, the result is[5]

$$-\mathrm{IP}_{\mathrm{corr}} = e_i + \sum_{j\neq i} e_{ji} + \sum_{j\neq i}\sum_{u} \frac{\langle ij\|iu\rangle^2}{e_u - e_j} + \frac{1}{2}\sum_{j\neq i}\sum_{k\neq i}\sum_{u} \frac{\langle jk\|iu\rangle^2}{e_i + e_u - e_j - e_k} \tag{10}$$

where

$$e_{ji} = \frac{1}{2}\sum_{u}\sum_{v} \frac{\langle ij\|uv\rangle^2}{e_i + e_j - e_u - e_v} \tag{11}$$

The summations involving j,k are over the occupied valence spin orbitals, and the summations involving u,v are over the Hartree–Fock virtual orbitals, excluding the same highest antibonding orbitals that were omitted from the CI orbital set mentioned above. The notation for the two-electron integrals is defined as[5]

$$\langle ab\|cd\rangle = \int \mathrm{d}1 \int \mathrm{d}2\; a(1)b(2)c(1)d(2)/r_{12} - \int \mathrm{d}1 \int \mathrm{d}2\; a(1)b(2)d(1)c(2)/r_{12}$$

The three terms involving summations on the right-hand side of eq 10 have been interpreted by Pickup and Goscinski.[5] The first sum accounts for the pair correlation energies which disappear upon removal of an electron from spin orbital i; the second sum accounts for the effects of reorganization of the remaining spin orbitals; and the third sum describes the changes in the remaining pair correlations due to the reorganization.

Method. All Hartree–Fock SCF calculations were carried out by using the GAUSSIAN 76 system of programs.[9] For the sulfur atoms, the 12s, 9p atom optimized basis set of Veillard[10] was contracted to 7s, 5p by a Raffenetti type of contraction scheme.[11,12] A single set of 3d functions ($\alpha_{3d} = 0.35$) was added. For H_2S_2, the set of functions referred to hereafter as the *valence basis set* consists of the above-described set for sulfur, the standard 3,1 split valence set for hydrogen, and bond functions at the midpoints of the bonds, $\alpha_{SS} = 0.6328$ and $\alpha_{SH} = 0.9562$. The exponents of the bond functions were optimized by calculations on H_2S and H_2S_2. For $(CH_3)_2S_2$, the *valence basis set* is slightly different and consists of the following: the sulfur basis set as described above; the 6-31G basis set for carbon;[13] and a minimal STO-6G basis for hydrogen.[13] For H_2S_2, the set of functions referred to hereafter as the *full basis set* consists of the valence basis set for H_2S_2, augmented by a single diffuse s function ($\alpha_s = 0.02$) and a set of diffuse p functions ($\alpha_p = 0.0133$). Addition of the diffuse functions allows the description of the lowest few Rydberg states as well as the valence states.

All configurations for which the coefficient λ_{nj} (eq 2) was greater than 0.05 were included in the zero-order part of the CI wave functions.

Table II. Optical Rotatory Strengths, Oscillator Strengths, and Excitation Energies for Dimethyl Disulfide

ϕ, deg	state	description	$10^{40}[R]^r$ ($10^{40}[R]^v$),[a] cgs	f	energy, eV
83.6[b]	1^1B	94% 13a → σ_{SS}*	27.4 (34.0)	0.0160	5.93
	2^1A	94% 12b → σ_{SS}*	−26.4 (−19.4)	0.0067	6.23
	2^1B	55% 13a → 'b' 40% 12b → 'b'	−34.6 (−44.3)	0.0110	7.66
	3^1A	63% 13a → 'a' 34% 12b → 'b'	13.0 (17.2)	0.0040	7.75
	B	62% 12a → 'b' 14% 13a → 'b' 23% 12b → 'a'	15.4 (23.4)	0.0948	8.94
	A	65% 12b → 'b' 28% 13a → 'a'	−124.2 (−162.6)	0.0500	9.22
	B	32% 13a → 'b' 31% 12a → 'b' 26% 12b → 'a'	287.2 (310.5)	0.5491	9.59
	A	95% 11b → 'b'	34.0 (35.3)	0.0226	10.21
	B	91% 12a → 'b'			
90	1^1B	93% 13a → σ_{SS}*	29.9 (36.9)	0.0170	6.02
	2^1A	96% 12b → σ_{SS}*	−21.6 (−15.7)	0.0059	6.03
	2^1B	55% 13a → 'b' 41% 12b → 'a'	−33.1 (−42.1)	0.0109	7.62
	3^1A	49% 13a → 'a' 47% 12b → 'b'	10.4 (15.5)	0.0062	7.72
	B	63% 12a → 'b' 22% 12b → 'a' 15% 13a → 'b'	14.1 (21.7)	0.0978	8.87
	A	51% 12b → 'b' 42% 13a → 'a'	−124.5 (−162.6)	0.0420	9.11
	B	33% 13a → 'b' 31% 12a → 'b' 25% 12b → 'a'	286.1 (311.0)	0.5293	9.51
	A	95% 11b → 'b'	33.8 (35.0)	0.0203	10.22
	B	89% 12a → 'b'	22.9 (24.0)	0.0523	10.71
100	2^1A	97% 12b → σ_{SS}*	−18.4 (−14.2)	0.0061	5.78
	1^1B	90% 13a → σ_{SS}*	36.2 (44.3)	0.0186	6.24
	3_1A	72% 12b → 'b' 25% 13a → 'a'	−0.7 (−0.9)	0.0137	7.62
	2^1B	51% 13a → 'b' 44% 12b → 'a'	−43.3 (−55.8)	0.0164	7.63
	B	64% 12a → 'b' 21% 12b → 'a' 15% 13a → 'b'	10.1 (16.3)	0.0987	8.84
	A	68% 13a → 'a' 26% 12b → 'b'	−103.8 (−135.3)	0.0245	9.18
	B	38% 13a → 'b' 31% 12a → 'b' 20% 12b → 'a'	291.6 (321.6)	0.4920	9.43
	A	95% 11b → 'b'	31.2 (31.9)	0.0179	10.32
	B	87% 12a → 'b'	12.8 (13.1)	0.0610	10.55

[a] Equation 9. [b] The experimental value.

Results and Discussion

Ground-State Properties. H_2S_2. H_2S_2 has been the subject of numerous semiempirical[1-3,14-19] and ab initio investigations,[20-31] most of which have involved geometry variation to some extent. In the majority of cases, particularly the ab initio studies, the calculated equilibrium geometry closely matches that determined experimentally (S–S = 2.055 Å, S–H = 1.327 Å, ∠SSH = 91.32°, ϕ = 90.6°)[32] and adopted in the present study. The HF-SCF energy of H_2S_2 at the experimentally determined geometry is −796.23280 hartrees, using the full basis set. This value is 0.003 hartree lower than that of Hinchliffe.[25] In Figure 2 is shown the variation of the SCF energy, dipole moment, and lower ionization

---

(6) (a) Reinhardt, W. P.; Doll, J. D. *J. Chem. Phys.* **1969**, *50*, 2767–2768. (b) Doll, J. D.; Reinhardt, W. P. *J. Chem. Phys.* **1972**, *57*, 1169–1184.

(7) Cederbaum, L. S.; Hohlneicher, G.; Peyerimhoff, S. *Chem. Phys. Lett.* **1971**, *11*, 421–424.

(8) Ecker, F.; Hohlneicher, G. *Theor. Chim. Acta* **1972**, *25*, 289–308.

(9) Binkeley, J. S.; Whitehead, R. A.; Hariharan, P. C.; Seeger, R.; Pople, J. A. *QCPE* **1978**, *11*, 368.

(10) Veillard, A. *Theor. Chim. Acta* **1968**, *12*, 405–411.

(11) Raffenetti, R. C. *J. Chem. Phys.* **1973**, *58*, 4452–4458.

(12) The contraction of the basis set was designed to conform with the general basis input limitations of the GAUSSIAN76 set of programs, the principal limitation being the maximum of six Gaussians per contracted basis function. Details of the contraction are available from the author on request. The Raffenetti contraction scheme, while very inefficient on the GAUSSIAN76 system, has the advantage of providing an excellent description of the core 1s, 2s, and 2p orbitals and thus allowing maximum flexibility in the valence region for the SCF and CI procedures with a limited number of basis functions.

(13) Hehre, W. J.; Ditchfield, R.; Pople, J. A. *J. Chem. Phys.* **1972**, *56*, 2257–2261.

(14) Boyd, D. B. *J. Am. Chem. Soc.* **1972**, *94*, 8799–8804.

(15) Yamabe, H.; Kato, H.; Yonezawa, T. *Bull. Chem. Soc. Jpn.* **1971**, *44*, 22–27.

(16) Yamabe, H.; Kato, H.; Yonezawa, T. *Bull. Chem. Soc. Jpn.* **1971**, *44*, 604–610.

(17) Woody, R. W. *Tetrahedron* **1973**, *29*, 1273–1283.

(18) Boyd, D. B. *J. Phys. Chem.* **1974**, *78*, 1554–1562.

(19) Synder, J. P.; Carlsen, L. *J. Am. Chem. Soc.* **1977**, *99*, 2931–2942.

(20) Schwartz, M. E. *J. Chem. Phys.* **1969**, *51*, 4182–4186.

(21) Veillard, A.; Demuynck, J. *Chem. Phys. Lett.* **1970**, *4*, 476–478.

(22) Hillier, I. H.; Saunders, V. R.; Wyatt, J. F. *Trans. Faraday Soc.* **1970**, *66*, 2665–2670.

(23) Davies, D. W. *Chem. Phys. Lett.* **1974**, *28*, 520–522.

(24) Blustin, P. H. *Theor. Chim. Acta* **1978**, *48*, 1–15.

(25) Hinchliffe, A. *J. Mol. Struct.* **1979**, *55*, 127–134.

(26) Ewig, C. S.; Mei, E. H.; Van Wazer, J. R. *Mol. Phys.* **1980**, *40*, 241–245.

(27) Trsic, M.; Laidlaw, W. G. *Int. J. Quantum Chem.* **1980**, *17*, 969–974.

(28) Takano, K.; Hosoya, H.; Iwata, S. *J. Am. Chem. Soc.* **1982**, *104*, 3998–4005.

(29) Pappas, J. A. *Chem. Phys.* **1976**, *12*, 397–405.

(30) Eslava, L. A.; Putnam, J. B.; Petersen, L. *Int. J. Pept. Protein Res.* **1978**, *11*, 149–153.

(31) Riga, J.; Verbist, J. J.; Lamotte, C.; Andre, J. M. *Bull. Soc. Chim. Belg.* **1978**, *87*, 163–170.

(32) Winnewisser, G.; Winnewisser, M.; Gordy, W. *J. Chem. Phys.* **1968**, *49*, 3465–3478.

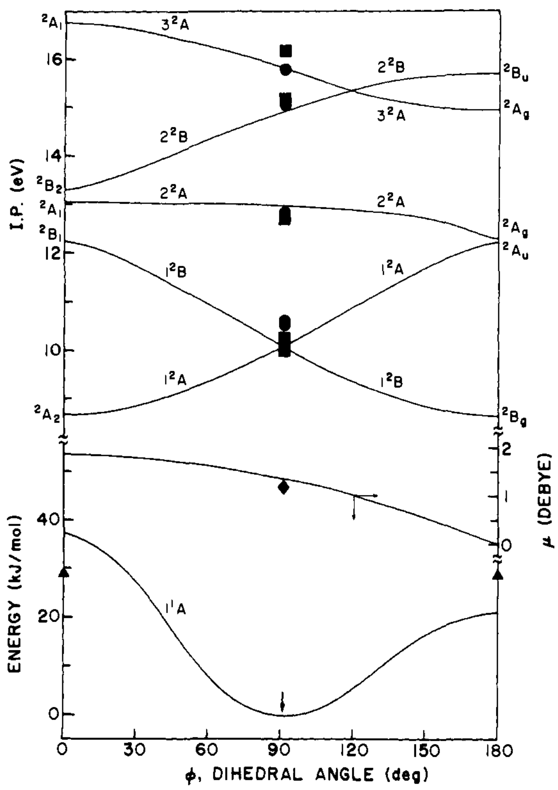

Figure 2. H_2S_2: Dihedral angle dependence of the HF-SCF energy, the calculated dipole moment, and the five lowest ionization potentials. The experimental values are taken from the following: (■) ref 35; (●) ref 36; (♦) ref 34; (▲) ref 33; (↓) ref 33.

potentials as a function of dihedral angle, ϕ. The experimental dihedral angle is very close to the extrapolated minimum, $\phi = 91.3°$.

The cis and trans barriers are calculated to be 37.7 and 21.7 kJ/mol, respectively, assuming rigid rotation about the S-S bond. An average value of 29 kJ/mol has been estimated from IR spectroscopic analysis.[33] Geometry relaxation tends to yield somewhat smaller values, particularly for the trans barrier.[20,26,29,30] Torsion about the S-S bond in acyclic disulfides requires less than a 5-kJ/mol expenditure of energy for a variation of 20° on either side of the equilibrium angle.

The dipole moment varies monotonically from 1.82 D for the cis structure to 0.0 D for the trans geometry. The equilibrium structure is calculated to have a dipole moment of 1.36 D, compared to the experimental value, 1.17 D.[34]

The lowest five ionization potentials (IP's), correct to second order in the many-body perturbation theory (eq 10), are shown in Figure 2. The corrections to Koopmans' theorem are small (~0.5 eV) and not strongly angle dependent. As a result, the dihedral angle dependence of the IP's closely mirrors the angular dependence of the molecular orbital (MO) energies, shown in Figure 1. Agreement of the computed values with experimental values[35,36] is quite good at $\phi = 90.6°$. The angular dependence matches that deduced from charge transfer spectra of a number of cyclic disulfides.[37] The lowest ^2A and ^2B molecular ion states cross at $\phi = 90°$. These arise from ionization of an electron from the MO's, 9a and 8b, respectively, which are composed of π bonding, n^+, and π antibonding, n^-, combinations of the sulfur 3p orbitals as shown in Figure 1. Ionization to the second lowest ^2A state is almost independent of ϕ. The energy of this state parallels the ground-state energy except in the range $120° \leq \phi \leq 180°$. The 2^2A state arises from ionization from MO 8a which is the in-phase combination of the sulfur nonbonded electron pair orbitals, both of which are tilted almost into alignment with the S-S bond. MO's 7a and 7b may best be described as symmetric and antisymmetric combinations of the S-H bonds, i.e., as $(\sigma_{SH})^+$ and $(\sigma_{SH})^-$, respectively. In the latter, the 3p orbitals of sulfur are polarized away from the hydrogen. The energies of these orbitals cross near $\phi = 120°$, as do the ionization potentials.

$(CH_3)_2S_2$. The HF-SCF energy of dimethyl disulfide at the experimentally determined geometry (S-S = 2.022 Å, C-S = 1.806 Å, C-H = 1.091 Å, ∠SSC = 104.1°, ∠SCH assumed tetrahedral, $\phi = 83.6°$)[38] is -874.24551 hartrees. Few ab initio calculations have been performed on this molecule.[29-31] Our SCF energy is lower by 0.32 hartree than that obtained by Pappas[29] using a large "double-ζ" basis set. From the three points computed in the present work ($\phi = 83.6°$, 90°, and 100°), one may extrapolate an equilibrium dihedral angle of 86.5°, which compares favorably with that of Pappas,[29] 86.2°, and the experimental value, 83.6°.

The calculated dipole moment, $u = 2.65$ D, is higher than the experimental value of 1.95 D.[39]

In Table I are given the experimental ionization potentials for $(CH_3)_2S_2$, together with the computed values both by Koopmans' theorem and after correction with use of eq 10 at the three dihedral angles considered. Agreement with the experimental values is very good, confirming the smaller than 90° dihedral angle in this compound and probably in other simple acyclic disulfides as well. As in the case of H_2S_2, the two highest occupied MO's, 13a and 12b, interchange near $\phi = 91°$, and their description is very close to that of 9a and 8b, shown in Figure 1. MO's 12a, 11b, and 11a also directly correspond to MO's 8a, 7b, and 7a of H_2S_2 (Figure 1), the latter two involving admixture of the S-C bonds comparable to the involvement of the S-H bond in H_2S_2. MO's 10b and 10a are combinations of the local e-type bond orbitals of the methyl groups, and little delocalization onto the sulfur atoms is apparent.

Excited States. As discussed above, the Bergson model[1,2,17] of the disulfide function predicts that the lowest two excited states should originate via excitation from the two highest occupied MO's, of symmetry a and b, into a low-lying σ_{SS}*, of symmetry b, thus giving rise to states of B and A symmetry. The former is lower in energy when $\phi < 90°$, the latter being lower when $\phi > 90°$. Since the σ_{SS}* orbital is relatively insensitive to ϕ, the angle dependence of the highest occupied MO's immediately offers an explanation of the observed bathochromic behavior of the lowest transition of disulfides[14] when ϕ is changed from 90°. There have been several investigations of the lower electronic states of disulfides by means of semiempirical calculations,[2,3,14,18,19] but no previous ab initio results are available. In Figure 3 is shown the correlation diagram for the angle dependence of the ground state and lower singlet excited states of H_2S_2 computed by using the full basis set. The lowest singlet excited state, 1^1B ($\phi < 90°$) or 2^1A ($\phi > 90°$), decreases in energy on either side of $\phi = 90°$. The second excited singlet state shifts to higher energy as ϕ shifts to values <90° until about $\phi = 70°$. At $\phi = 70°$, an avoided crossing occurs and the second excited single state, like the first, decreases in energy as ϕ is decreased to 0°. The decrease in energy of the second excited state is contrary to the Bergson model but agrees with experiment and was anticipated by some CNDO/CI calculations.[3,19] The same phenomenon occurs when ϕ is greater than 90°, the avoided crossing being near $\phi = 120°$.

The expectation values, $\langle\phi_u|r^2|\phi_u\rangle$ $(=\langle r^2\rangle)$ are displayed in Figure 3. These provide a measure of the magnitude of the terminal orbital of the excitation, ϕ_u, and therefore of the spatial dimensions of the excited state. The lowest excited state has $\langle r^2\rangle \simeq 15$ bohr,[2] indicative of a valence excited state. The states calculated to occur above 6.5 eV all have substantially larger values of $\langle r^2\rangle$ and are Rydberg states. In the vicinity of $\phi = 90°$ the second excited state also is clearly valence in character, but on

---

(33) Redington, R. L. *J. Mol. Spectrosc.* **1962**, *9*, 469-476.

(34) Smyth, C. P.; Lewis, G. L.; Grossman, A. J.; Jennings F. B., III *J. Am. Chem. Soc.* **1940**, *62*, 1219-1223.

(35) Wagner, G.; Bock, H. *Chem. Ber.* **1974**, *107*, 68-77.

(36) Solouki, B.; Bock, H. *Inorg. Chem.* **1977**, *16*, 665-669.

(37) Moreau, W. M.; Weiss, K. *J. Am. Chem. Soc.* **1966**, *88*, 204-210.

(38) Beagley, B.; McAloon, K. T. *Trans. Faraday Soc.* **1971**, *67*, 3216.

(39) Kushner, L. M.; Gorin, G.; Smyth, C. P. *J. Am. Chem. Soc.* **1950**, *72*, 477-479.

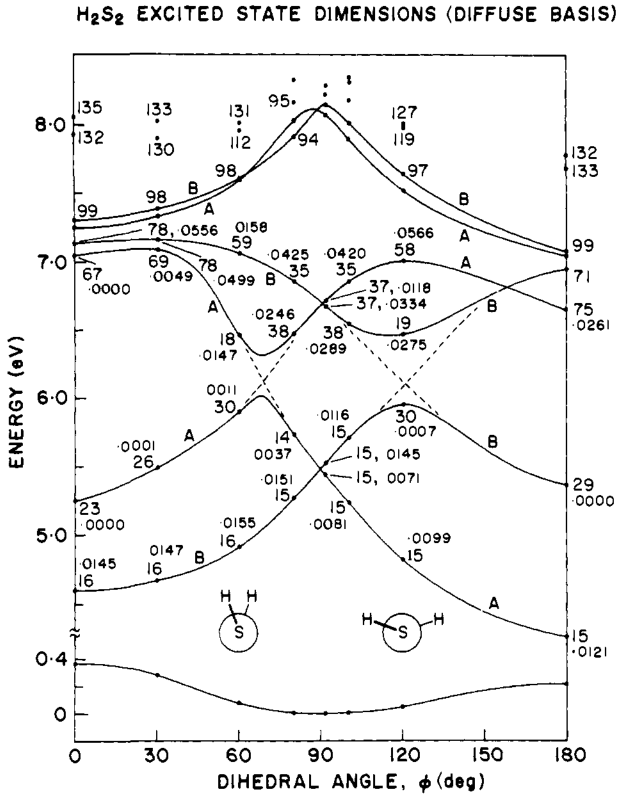

Figure 3. State-correlation diagram for H_2S_2 using the full basis set. 1^1A is the ground state. The points denote the geometries at which computations were performed. The whole numbers are $\langle\phi_u|r^2|\phi_u\rangle$, in units of bohr,[2] where ϕ_u is the terminal orbital of the largest component of the CI expansion of the state. The four-digit decimal numbers are the values of the oscillator strength, f.

the other side of either avoided crossing, $\phi < 70°$ or $\phi > 120°$, the prinicipal component of the state is more diffuse. The terminal orbital correlates with the in-phase combination of the two S–H antibonding group orbitals, $(\sigma_{SH}^*)^+$, which transforms as a_1 or b_u at the extrema, $\phi = 0°$ or $\phi = 180°$, respectively. The CI description of the state is unambiguously $n^- \rightarrow (\sigma_{SH}^*)^+$ or 9a → 'a' ($2a_2 \rightarrow$ 'a_1' for $\phi = 0°$) in the two planar geometries. Near $\phi \leq 90°$, the second excited singlet state is described as expected from the Bergson model, $n^+ \rightarrow \sigma_{SS}^*$, or 8b → 'b'. The two configurations mix strongly at dihedral angles near 70°. This state is truly a "mixed valence Rydberg state" because the two principal configurations vary significantly in the spatial extension of the terminal orbitals, $(\sigma_{SH}^*)^+$ being much more diffuse than σ_{SS}^*. The explicit composition of the second excited singlet state has important consequences for its computed optical activity as discussed below.

In Figure 3, the ϕ dependence of the calculated oscillator strength is shown. Contrary to previous calculations,[3,18,19] the oscillator strength of the lowest wavelength transition does not change much when ϕ is changed from 0° to 80°, and the second transition gains little intensity in this range. The observed intensity at the equilibrium geometry of acyclic disulfides would be due to the sum of two nearly degenerate transitions (total $f = 0.0216$) and would appear somewhat larger than the intensity of the lowest band at $\phi < 90°$ or $\phi > 90°$.

The calculated excitation energy, 5.45 eV, for the longest wavelength transition for H_2S_2 is about 0.64 eV higher than observed, 4.81 eV.[40] For $(CH_3)_2S_2$, the greater discprepancy between computed, 5.93 eV, and observed, 4.85 eV[40]–4.96 eV,[41] is a reflection of the more restricted C and H basis used. The lack of diffuse functions on S is not a limitation, since by using the valence basis set of H_2S_2 the computed excitation energies at $\phi = 90.6°$ for the first two transitions, 5.48 and 5.55 eV, respectively, are only marginally higher than when the full basis set is used, 5.45 and 5.52 eV, respectively. This result confirms the valence nature of the 2^1A ($n^+ \rightarrow \sigma_{SS}^*$) and 1^1B ($n^- \rightarrow \sigma_{SS}^*$) states in the vicinity of $\phi = 90°$.

Computed transition properties, $[R]$, f, and ΔE, for $(CH_3)_2S_2$ are given in Table II. The broad first transition of $(CH_3)_2S_2$, placed at 4.85 eV[40] or 4.96 eV,[41] with an estimated oscillator strength, $f = 0.0312$,[41] was suggested to consist of two overlapping transitions.[41] These are the valence states 1^1B ($n^- \rightarrow \sigma_{SS}^*$) and 2^1A ($n^+ \rightarrow \sigma_{SS}^*$) separated by 0.3 eV, with a combined intensity of $f = 0.0160 + 0.0067 = 0.0227$.

Two other transitions have been identified in the UV spectrum of $(CH_3)_2S_2$,[41] a shoulder at 5.89 eV, $f = 0.028$, and a strong band at 6.36 eV, $f = 0.303$. The present calculations indicate that the 5.89-eV band also is a composite band, the result of overlapping of two nearly degenerate transitions, $1^1A \rightarrow 2^1B$ and $1^1A \rightarrow 3^1A$. The states, 2^1B and 3^1A, are themselves composite in character, each being an admixture principally of two configurations which are generated by excitation of an electron from one of the two nearly degenerate MO's, 13a or 12b, into a linear combination of the two S–C antibonding orbitals, $(\sigma_{SC}^*)^+$ or $(\sigma_{SC}^*)^-$, as appropriate for the symmetry of the state. The S–C antibonding orbitals are not optimally described with the valence basis set. Comparison of the excitation energies for the corresponding transitions in H_2S_2, calculated with the valence and full basis sets, reveals that the transition energy is lowerd by 0.9 eV, from 7.56 to 6.68 eV, when diffuse s and p functions are added to the basis set of S. Addition of diffuse functions also increases the total oscillator strength of the two transitions from $f = 0.0243$ ($f = 0.0160$ for $(CH_3)_2S_2$) to $f = 0.0666$. Experimentally, this band, which appears as a shoulder on the side of the stronger band at shorter wavelength, diappears in solution. This is consistent with the calculated diffuse nature of the 2^1B and 3^1A states near $\phi = 90°$.

The stronger band at 6.36 eV, $f = 0.303$,[41] in $(CH_3)_2S_2$ in the gas phase, is blue shifted and decreased in intensity as the solvent polarity is increased. The computations on H_2S_2, using the full basis set, do not suggest any single electronic state as a candidate for this band. Indeed, within 0.5 eV of the fifth transition, at 8.08 eV, are predicted to occur six more, with a combined oscillator strength, $f = 0.128$. All of these originate from either n^+ or n^- (9a or 8b) and terminate in linear combinations of the diffuse s and p functions of the set. In other words, the third band of acyclic disulfides, at 6.36 eV, is composed of multiple transitions to Rybderg states. The shortfall in the total oscillator strength of these transitions suggests that there should be an additional component not calculated to occur in the low-energy part of the spectrum. The first single transition with appreciable oscillator strength, $f = 0.8835$, corresponds largely to 8a → 'b' ($\sigma_{SS} \rightarrow \sigma_{SS}^*$) and is calculated to occur at 8.86 eV. With the valence basis set, for H_2S_2 and $(CH_3)_2S_2$, this transition occurs at 9.32 and 9.59 eV, respectively, with $f = 0.6602$ and $f = 0.5491$, respectively. It is plausible that the $\sigma_{SS} \rightarrow \sigma_{SS}^*$ transition contributes to the intensity observed at 6.36 eV in spite of the 2.5–3 eV discrepancy in excitation energy. As noted above, the Rydberg transitions alone do not accumulate enough intensity. In addition, the nature of the transition, which removes an electron from the S–S bonding orbital and places it into the S–S antibonding orbital, will render it very nonvertical and broad, if not dissociative.

Optical Activity of Disulfides. The calculated optical rotatory strengths for the lower electronic transitions of the disulfide chromophore are shown in Figures 4 and 5, superimposed on the state correlation diagram for H_2S_2, and are given in Table II for $(CH_3)_2S_2$. The figures differ in that the former displays results obtained with the full basis set while for the latter the valence basis was used. The reason for discussing both sets of results will be explained in the discussion below. The energetics of the correlation diagram have been discussed above in connection with Figure 3 and will not be repeated here in detail.

Cyclic Disulfides. The rotatory strength of the lowest transition decreases in absolute magnitude as ϕ is varied away from 90°,

---

[40] Feher, F.; Munzner, H. *Chem. Ber.* **1963**, *96*, 1131–1155.

[41] Thompson, S. D.; Carroll, D. G.; Watson, F.; O'Donnell, M.; McGlynn, S. P. *J. Chem. Phys.* **1966**, *45*, 1367–1379.

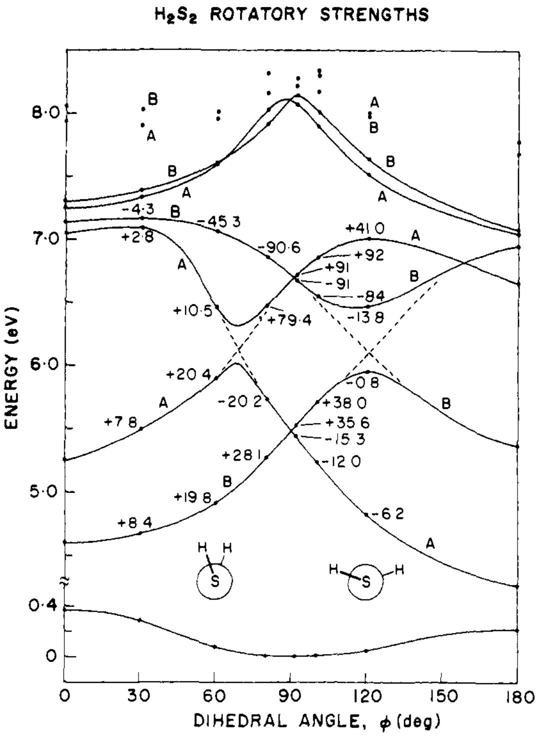

Figure 4. State-correlation diagram for H_2S_2 using the full basis set. The numbers at the points are the values of the rotatory strength, $[R]^r \times 10^{-40}$ cgs, of the transitions at the geometries indicated by the points.

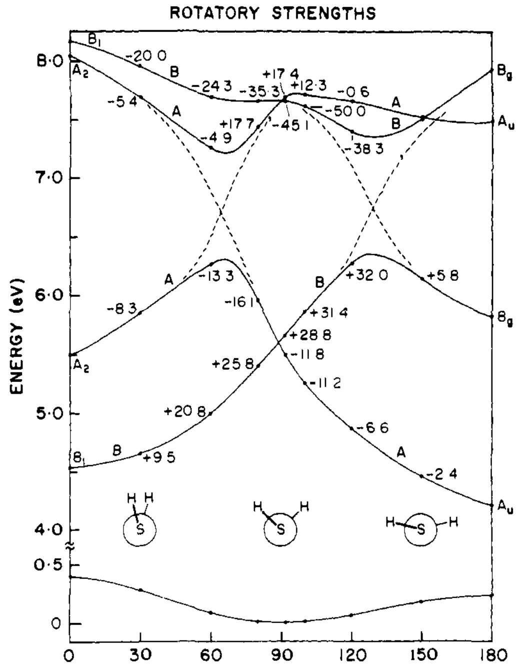

Figure 5. State-correlation diagram for H_2S_2 using the valence basis set. The numbers at the points are the values of the rotatory strength, $[R]^r \times 10^{-40}$ cgs.

and the signs vary in the manner deduced by Linderberg and Michl[2] on the basis of the Bergson model[1] and observed experimentally for angularly constrained disulfides.[42-46] The signs of the lowest energy transition are consistent with the known absolute configuration of twisted disulfides[47,48] and the empirical rule of disulfide chirality formulated for 1,2-dithianes first by Carmack and Neubert.[42,43]

Experimentally,[42-44] 1,2-dithianes with a right-handed twist (P chirality) of the disulfide bond exhibit a strong positive Cotton effect, $[R] \simeq +20 \times 10^{-40}$ cgs, for the first band, which occurs at 290 nm (4.28 eV). The second band around 240 nm (5.17 eV) is of opposite sign and more sensitive to minor perturbations. The S–S dihedral angle in 1,2-dithianes is about 60°. In disulfides where the dihedral angle is constrained to about 30°, the same observations are made except that the bands are of half the intensity and are red shifted.[44] Inspection of Figure 4 reveals that the signs of the rotational strengths of the second transition of H_2S_2, $1^1A \rightarrow 2^1A$, in the range $\phi < 70°$, computed with the full basis set, are *not* in agreement with experimental observations on larger disulfides. In Figure 5 is shown the same information as in Figure 4, but computed by using the valence basis set. Qualitatively, the correlation diagrams are the same for the first two states, as are the computed rotatory strengths, except the sign of the rotatory strength of the $1^1A \rightarrow 2^1A$ transition at $\phi < 70°$ is opposite to that shown in Figure 4 and is now in agreement with experimental observations.

We wish to suggest that the above-mentioned changeover in sign with the change of basis set is telling us something of the nature of the second electronic state in disulfides. The 2^1A state near $\phi = 70°$ arises from the avoided crossing of two very different electronic configurations, the valence configuration, 8a → 'b' ($n^+ \rightarrow \sigma_{SS}{}^*$), which dominates the description of 2^1A for $\phi > 90°$, and the more diffuse Rydberg configuration, 9a → 'a' ($n^- \rightarrow (\sigma_{SH}{}^*)^+$), which is the limiting configuration 2^1A as $\phi \rightarrow 0°$. The extent to which two configurations are mixed depends on the energy separation which is strongly dihedral angle dependent. The configuration 9a → 'a' ($n^- \rightarrow (\sigma_{SS}{}^*)^+$) is lower in energy at $\phi = 0°$, and it increases rapidly in energy as ϕ increases. The other configuration, 8b → 'b' ($n^+ \rightarrow \sigma_{SS}{}^*$), is much higher in energy when $\phi = 0°$, but it decreases in energy rapidly as ϕ increases and crosses the first near $\phi = 70°$. Inspection of the CI wave function obtained by using the full basis set which allows both configurations to be optimally described reveals that at $\phi = 60°$, 2^1A consists 90% of the diffuse configuration, 9a → 'a' ($\langle r^2 \rangle = 34.0$ bohr^2), and 9% of the valence configuration, 8b → 'b' ($\langle r^2 \rangle = 12.5$ bohr^2). At $\phi = 30°$, the proportion of the diffuse component has increased to 95%. These results and those shown in Figure 4 apply to H_2S_2 in the gas phase. One may enquire as to the consequences to the 2^1A state when the molecule is placed in solution. It is conceptually appealing to imagine that the "valence part" of the state is relatively unaffected by the dense medium but that the "part that wants to be diffuse" is compressed and shifted to higher energy. Put another way, the state description resembles more the compact part, 8b → 'b', and less the "diffuse" part, 9a → 'a', and the latter would itself be compressed by the van der Waals cage of the solvent.

Under certain circumstances, such as those described above, a more realistic description of the electronic configuration of a molecule in solution, or perhaps a much larger related molecule even in the gas phase, may be obtained with a basis set which forces compression of the diffuse components of the electronic states. Thus, use of the valence basis set gives a qualitatively different picture of the 2^1A state in "in solution", when $\phi < 70°$. At $\phi = 30°$, the configuration 9a → 'a' ($n^- \rightarrow (\sigma_{SH}{}^*)+$) still dominates the description of 2^1A, but its proportion has decreased to 90% and the terminal MO, $(\sigma_{SH}{}^*)^+$, is more compact, $\langle r^2 \rangle = 13.6$ bohr^2. At $\phi = 60°$, this configuration comprises 36% of 2^1A,

---

(42) Carmack, M.; Neubert, L. A. *J. Am. Chem. Soc.* **1967**, *89*, 7134–7136.

(43) (a) Claeson, G. *Acta Chem. Scand.* **1968**, *22*, 2429–2437. (b) Dodson, R. M.; Nelson, V. C. *J. Org. Chem.* **1968**, *33*, 3966–3968; **1952**, *18*, 2549–2555.

(44) Neubert, L. A.; Carmack, M. *J. Am. Chem. Soc.* **1974**, *96*, 943–945.

(45) Ludescher, U.; Schwyzer, R. *Helv. Chim. Acta* **1976**, *54*, 1637–1644.

(46) Kukolja, S.; Demarco, P. V.; Jones, N. D.; Chaney, M. O.; Paschal, J. W. *J. Am. Chem. Soc.* **1972**, *94*, 7592–7593.

(47) (a) Beecham, A. F.; Fridrichsons, J.; Mathieson, A. McL. *Tetrahedron Lett.* **1966**, 3131–3138. (b) Beecham, A. F.; Mathieson, A. McL. *Tetrahedron Lett.* **1966**, 3139–3146. (c) Fridrichsons, J.; Mathieson, A. McL. *Acta Crystallogr.* **1967**, *23*, 439–448.

(48) Nagarajan, R.; Neuss, N.; Marsh, M. M. *J. Am. Chem. Soc.* **1968**, *90*, 6518–6519.

with 62% consisting of 8b → 'b' (n$^+$ → σ_{SS}^*). The most dramatic visible consequence is that the rotatory strength of the $1^1A \rightarrow 2^1A$ transition is negative, in agreement with experiment. Very similar results are obtained for $(CH_3)_2S_2$ (Table II), for which it was only possible to use a valence basis set. One can question whether the observed sensitivity of the second CD band of cyclic disulfides to minor perturbations[42] may be due in part to the delicate balance of the two distinct components of that state in the vicinity of the avoided crossing. Experimental data in the gas phase have been reported for only one optically active disulfide, **1**,[44] in which the dihedral angle is less than the predicted crossover point. While

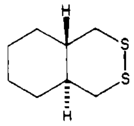

1

the CD spectrum was not published and no information on the relative intensities of the first two CD bands was presented, it was implicit that the sign of the second CD band is opposite to that of the first, as it is in various hydrocarbon and hydroxylic solvents. It is to be hoped that the above discussion will spur the preparation of smaller disulfides with constrained dihedral angles for which the chiroptical properties of the second transition can be tested.

Besides the transitions at 290 and 240 nm, Neubert and Carmack[44] have identified four more transitions, at 216, 206, 196, and 188 nm, which were found in a series of model cyclic disulfides, including **1**. Since transitions due to other chromophores and even C–C skeletal transitions may interfere in the shorter wavelength region of the spectrum, it may not be appropriate to attempt to search for the explanation of their optical activity on the basis of the simple model compounds used in the present study. However, there is an intense UV transition near 195 nm (6.4 eV) which appears in both cyclic and acyclic disulfides and which was identified above as having a contribution from the $\sigma_{SS} \rightarrow \sigma_{SS}^*$ transition. Experimentally, the sign of the Cotton effect is the same as that of the first transition. Computationally, the rotatory strengths of the two states which have most significant $\sigma_{SS} \rightarrow \sigma_{SS}^*$ character, numbers 5 and 7 in Table II, both have positive rotatory strength for a disulfide with P chirality. A very large value is predicted for the second of the two. The sign is independent of whether ϕ is greater or less than 90°. Transition 6 of Table II, which involves n → σ_{SC}^* components of A symmetry, has a large negative rotatory strength less than half the intensity of the oppositely signed seventh transition which is less than 0.4 eV away. If the magnitude of the rotatory strength of the $\sigma_{SS} \rightarrow \sigma_{SS}^*$ is as large as computed relative to other Cotton effects in the same region of the spectrum, it is possible that the net rotatory strength observed in this region (<190 nm) will be determined by it.

Acyclic Disulfides. The reduced optical activity characteristic of acyclic disulfides whose dihedral angles are close to 90° and which can undergo the conformational change, P-2 ⇌ M-2, may be rationalized in two ways. The two structures, P-2 and M-2, are antipodal in the chromophore, the S–S unit. Thus disulfides,

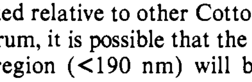

P-2   M-2

though chiral, are optically inactive and unresolvable if neither of the two substituents is chiral. When one or both substituents is chiral, the structures, P-2 and M-2, are diastereomeric and one of the two will be favored. As described earlier, barriers to the hindered rotation are sufficiently low that P-2 and M-2 cannot be separated in solution or in the gas phase. If there is not much chiral discrimination due to intramolecular interactions, then the observed low optical activity may simply be due to cancellation arising from only a small "enantiotopic" excess of P-2 or M-2. However, the Bergson model,[1] as applied by Linderberg and Michl,[2] offers an additional mechanism which hinges on the fact that ϕ is close to 90°, since at this geometry, the equal in magnitude but oppositely signed rotational strengths of two degenerate transitions of A and B symmetry cancel each other. Considerable effort,[30,49-52] much of it centred on L-cystine, **3**,[30,49-51] has been expended to sort out the interrelationship between the two phenomena.

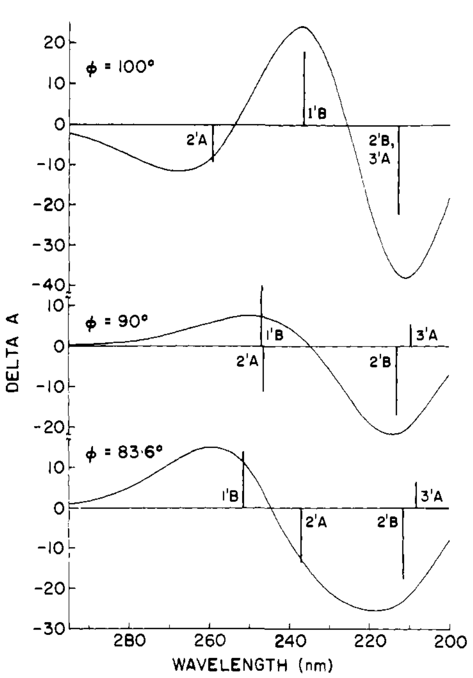

Figure 6. Calculated CD spectra of dialkyl disulfides at three values of the S–S dihedral angle, ϕ. Gaussian line shapes whose areas correspond to the calculated rotatory strengths for $(CH_3)_2S_2$ (width at half-height = 0.67 eV) were centered on the transition energies. The quantity 1.0 eV was substracted from the calculated transition energies for the first and second transitions of $(CH_3)_2S_2$ (Table II), and 1.6 eV from the third and fourth, in order to correspond to the experimental values. The vertical bars at the transition wavelengths are proportional to the values of $[R]^r$.

A thorough analysis by NMR and CD spectroscopy, carried out by Casey and Martin,[51] concluded that the observed optical activity of **3** is *not* due to any significant preference for either the P or the M form, but rather due to differing rotameric populations about single bonds other than the S–S bond. Prediction of the optical activity due to asymmetric perturbations not directly reflected on the chirality of the S–S linkage, as are evidently important in **3**,[49,51] is beyond the scope of the present study.

The rotatory strengths given in Figure 4 or Figure 5 or Table II indicate that, while near ϕ = 90°, the signs of the CD of the first two transitions are opposite and the $1^1A \rightarrow 1^1B$ transition has greater intensity than the $1^1A \rightarrow 2^1A$ transition. Thus complete cancellation of the rotatory strength near ϕ = 90° will not take place. The simulated CD spectra for an acyclic disulfide of P chirality, using the data for $(CH_3)_2S_2$ at the three values for ϕ, are shown in Figure 6. The CD spectra at ϕ = 83.6° and ϕ = 90° are deceptively simple. Although four transitions are present, only two CD bands are apparent. At ϕ = 90°, the transitions occur as nearly degenerate pairs and the contribution of the weaker transition of each pair is completely masked. At ϕ = 83.6°, the second and third bands, which have the same Cotton effect, have merged. Notice that it would *not* be possible to assign excitation energies from the CD spectrum in this case.

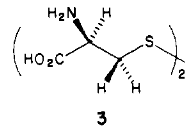

3

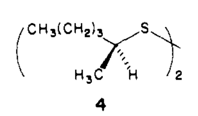

4

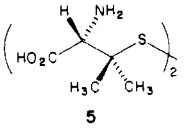

5

---

(49) Coleman, D. L.; Blout, E. R. *J. Am. Chem. Soc.* **1968**, *90*, 2405–2416.
(50) Mattice, W. L. *J. Am. Chem. Soc.* **1977**, *99*, 2324–2330.
(51) Casey, J. P.; Martin, R. B. *J. Am. Chem. Soc.* **1972**, *94*, 6141–6151.

While neither form, P-2 nor M-2, of **3** is preferred,[51] the same may not be true of acyclic disulfides where the substituents directly attached to S are larger than CH_2R. (*S*,*S*)-Bis(1-methylbutyl)disulfide (**4**) exhibits weak positive ($\Delta\epsilon = +0.09$) and negative ($\Delta\epsilon = -0.05$) CD bands at 270 and 238 nm, respectively, in *n*-heptane.[51] The crossover point, 251 nm, coincides with the UV maximum at 252 nm ($\epsilon = 400$). A second crossover point occurs at 234 nm. While **4** undoubtedly exists in several rotameric conformations, the gross characteristics of its CD spectrum resemble the $\phi = 100°$ curve of Figure 6 and therefor are consistent with **4** having preferentially adopted the P conformation with a dihedral angle greater than 90°.

The CD spectrum of D-penicillamine disulfide (**5**) in water has a broad negative band ($\Delta\epsilon = -0.2$) with $\lambda_{max} = 262$ nm.[51] The CD is almost zero at 230 nm but does not change sign. A second negative peak ($\Delta\epsilon = -0.4$) is observed at 220 nm. There is no UV maximum which corresponds to the CD band at 262 nm. The data for **5** are consistent with **5** having a right-handed twist (P chirality) and an S–S twist angle greater than 90°. If, as suggested by molecular machanics calculations on the structurally similar di-*tert*-butyl disulfide,[53] the angle is in excess of 110°, then the lack of UV absorption may be attributable to the predicted low oscillator strength for the $1^1A \rightarrow 2^1A$ transition. The second CD band, which is calculated to be positive and stronger than the first, would be buried under the CD band due to the carboxylate group which occurs at 220 nm.[51]

Acknowledgment. I thank the Natural Sciences and Engineering Research Council of Canada for continuing financial support. The receipt of large amounts of computing time at modest cost from the University of Calgary is gratefully appreciated. The assistance of Scott Collins in the development of the basis sets was of great value.

Registry No. H_2S_2, 13465-07-1; $(CH_3)_2S_2$, 624-92-0.

---

(52) Szantay, C.; Kotick, M. P.; Shefter, E.; Bardos, T. J. *J. Am. Chem. Soc.* **1967**, *89*, 713–714.

(53) Joergensen, F. S.; Snyder, J. P. *Tetrahedron* **1979**, *35*, 1399–1407.

Excited-State Dipole Moment and Solvatochromism of Highly Fluorescent Rod-Shaped Bichromophoric Molecules

Ger F. Mes, Bettina de Jong, Hendrik J. van Ramesdonk, Jan W. Verhoeven,* John M. Warman,* Matthijs P. de Haas, and Leny E. W. Horsman-van den Dool

Contribution from the Laboratory for Organic Chemistry, University of Amsterdam, Nieuwe Achtergracht 129, 1018 WS Amsterdam, The Netherlands, and Interuniversity Reactor Institute, Mekelweg 15, 2629 JB Delft, The Netherlands. *Received March 5, 1984*

Abstract: Efficient photoinduced charge separation can occur in molecules containing electron donor (D) and acceptor (A) groups separated by an elongated paraffinic spacer. For two molecules of this type the dipole moment of the excited state thus achieved (D^+–A^-) is shown to be as high as 25 ± 2 D via nanosecond time-resolved microwave conductivity measurements. Despite the lack of either direct D/A contact or coupling via a π-electron system the dipolar excited states are found to emit charge-transfer-type fluorescence with a quantum yield exceeding 50% in some solvents. The enormous solvatochromism of this fluorescence makes these molecules attractive as fluorescent polarity probes.

Photoinduced charge separation and migration play a key role in many important photochemical and photophysical processes including photosynthesis.[1] Much information regarding the geometrical requirements for electron-transfer between donor (D) and acceptor (A) species has been acquired from the study of bichromophoric systems incorporating D and A chromophores connected by one or more paraffinic moieties which restrict the D/A separation and orientation. Often the paraffinic moieties allow[2] or even enforce[3,4] close contact of the D and A chromophores (type I in Figure 1), thus mimicing the general situation found in intermolecular complexes and exciplexes.[5] We[6–8] and others[9–11] have shown, however, that (photoinduced) intramolecular electron transfer may also occur if a paraffinic spacer enforces a rod-like molecular shape with D and A located at opposite ends (type II in Figure 1).

In I the D/A interaction occurs essentially via direct through-space overlap, while in II through-bond interaction via the σ framework of the spacer plays an important role.[6,7,12] For both I and II the lowest excited singlet state may acquire extensive charge-transfer (CT) character (i.e., D^+A^-), leading to pronounced solvatochromism of any fluorescence ($\tilde{\nu}_{ct}$) resulting from it. If

---

* J.W.V.: University of Amsterdam. J.M.W.: Interuniversity Reactor Institute.

(1) Jortner, J. *J. Am. Chem. Soc.* **1980**, *102*, 6676–6686.

(2) For a review see: Schryver, F. C. de.; Boens, N.; Put, J. *Adv. Photochem.* **1977**, *10*, 359–465.

(3) Borkent, J. H.; Verhoeven, J. W.; de Boer, Th. J. *Chem. Phys. Lett.* **1976**, *42*, 50–53.

(4) Overfield, R. E.; Scherz, A.; Kaufmann, K. J.; Wasielewski, M. R. *J. Am. Chem. Soc.* **1983**, *105*, 5747–5752.

(5) "The Exciplex"; Gordon, M., Ware, W. R., Eds.; Academic Press: New York, 1975.

(6) Pasman, P.; Verhoeven, J. W.; de Boer, Th. J. *Chem. Phys. Lett.* **1978**, *59*, 381–385.

(7) Pasman, P.; Rob, F.; Verhoeven, J. W. *J. Am. Chem. Soc.* **1982**, *104*, 5127–5133.

(8) Pasman, P.; Koper, N. W.; Verhoeven, J. W. *Recl. Trav. Chim. Pays-Bas* **1982**, *101*, 363–364.

(9) Davidson, R. S.; Bonneau, R.; Joussot-Dubien, J.; Toyne, K. J. *Chem. Phys. Lett.* **1979**, *63*, 269–272.

(10) Calcaterra, L. T.; Closs, G. L.; Miller, J. R. *J. Am. Chem. Soc.* **1983**, *105*, 670–671.

(11) Stein, C. A.; Lewis, N. A.; Seitz, G. *J. Am. Chem. Soc.* **1982**, *104*, 2596–2599.

(12) Baker, A. D.; Scharfman, R.; Stein, C. A. *Tetrahedron Lett.* **1983**, *24*, 2957–2960.

0002-7863/84/1506-6524$01.50/0